Brain-Penetrant Tetrahydronaphthalene Thromboxane A2-Prostanoid (TP) Receptor Antagonists as Prototype Therapeutics for Alzheimer's Disease

James H. Soper,[†,§] Shimpei Sugiyama,[‡,§] Katie Herbst-Robinson,[†,§] Michael J. James,[†] Xiaozhao Wang,[‡] John Q. Trojanowski,[†] Amos B. Smith, III,[‡] Virginia M.-Y. Lee,[†] Carlo Ballatore,[†,‡] and Kurt R. Brunden*,[†]

[†]Center for Neurodegenerative Disease Research, Institute on Aging, Perlman School of Medicine, University of Pennsylvania, 3600 Spruce Street, Philadelphia, Pennsylvania, 19104-6323

[‡]Department of Chemistry, School of Arts and Sciences, University of Pennsylvania, 231 South 34th Street, Philadelphia, Pennsylvania, 19104-6323

ABSTRACT: A hallmark pathological feature of the Alzheimer's disease (AD) brain is the presence of senile plaques, which comprise amyloid β (Aβ) peptides that are derived from the amyloid precursor protein (APP). The plaque-containing AD brain is thought to be under oxidative stress, as evidenced by increased lipid oxidation products that include isoprostane-F2αIII (iPF2αIII). IPF2αIII can bind to and activate the thromboxane A2-prostanoid (TP) receptor, and TP receptor activation causes increased Aβ production through enhancement of APP mRNA stability. Moreover, TP receptor antagonists have been shown to block iPF2αIII-induced increases of Aβ secretion. Thus, the TP receptor may be a potential drug target for AD therapy. However, here we show that existing TP receptor antagonists have poor blood-brain barrier (BBB) permeability, likely due to the presence of a carboxylic acid moiety that is believed to be important for receptor interaction, but which may hamper passive diffusion across the BBB. We now report selected analogues of a known tetrahydronaphthalene TP receptor antagonist, wherein the carboxylic acid moiety has been replaced by heterocyclic bioisosteres. These heterocyclic analogues retained relatively high affinity for the mouse and human TP receptors, and, unlike the parent carboxylic acid compound, several examples freely diffused across the BBB into the brain upon administration to mice. These results reveal that brain-penetrant tetrahydronaphthalene TP receptor antagonists can be developed by substituting the carboxylic acid moiety with a suitable nonacidic bioisostere. Compounds of this type hold promise as potential lead structures to develop drug candidates for the treatment of AD.

KEYWORDS: Alzheimer's disease, amyloid precursor protein, antagonist, blood-brain barrier, plaques, thromboxane receptor
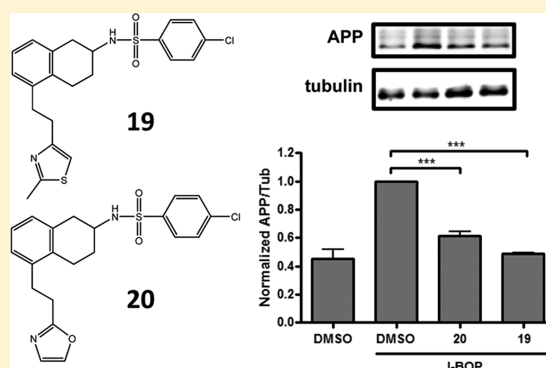
Alzheimer's disease (AD) is the most common cause of dementia in elderly populations, affecting approximately 10% of individuals over age 65.[1,2] The AD brain is characterized by overt neurodegeneration[3] and the presence of senile plaques comprising insoluble fibrils of Aβ peptides which are produced through sequential proteolytic cleavage of the amyloid precursor protein (APP).[4] A second pathological hallmark of the AD brain is the occurrence of intracellular inclusions composed of hyperphosphorylated tau proteins.[5,6] Familial forms of AD can be caused by mutations in APP that result in increased proteolytic generation of amyloidogenic Aβ peptides, as well as by mutations in the presenilin proteins that are required for the proteolytic processing of APP to yield Aβ.[7−10] These genetic data provide compelling support for the "amyloid" hypothesis, which postulates that it is the production of Aβ that drives disease pathogenesis in AD. Accordingly, there is significant interest in identifying therapeutic strategies that will lead to decreased Aβ production, and there are ongoing efforts to identify inhibitors of the enzymes that generate Aβ.[11,12]

A consequence of Aβ plaque deposition in the AD brain appears to be the onset of oxidative stress, as evidenced by the generation of oxidized lipids.[13,14] These include the F2α-isoprostanes (iPF2α) that result from nonenzymatic lipid peroxidation of arachidonic acid, with elevated iPF2α levels in brain and cerebrospinal fluid of AD patients, as well as in patients with mild cognitive impairment.[15−17] Increased generation of iPF2α has also been reported in the brain of the Tg2576 mouse model of AD, which expresses mutated human APP, with the elevation of these oxidized lipids
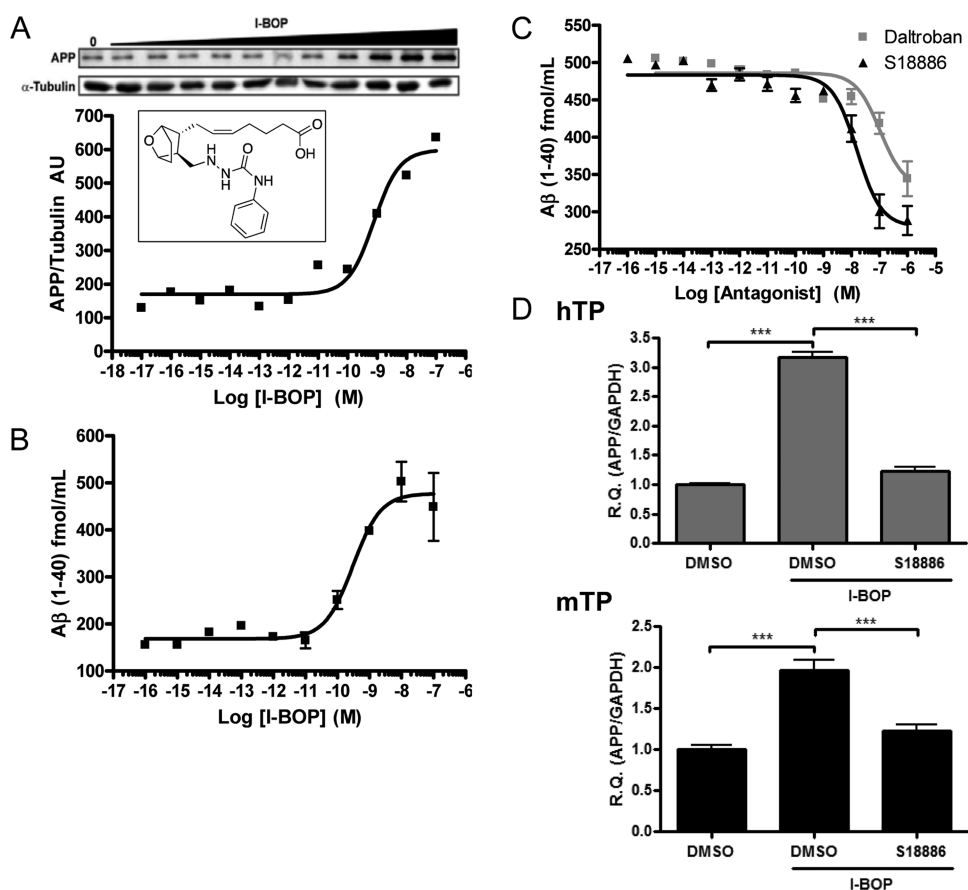
Figure 1. TP receptor activation increases APP protein levels, Aβ secretion and APP mRNA. (A) Activation of the hTP receptor with I-BOP (structure shown in inset) increases APP protein levels, as demonstrated by Western blot and quantified by densitometric analysis of the ratio of APP/α-tubulin. HEK293 cells stably coexpressing hAPP and hTP receptor were treated with I-BOP at the indicated concentrations. (B) Activation of the hTP receptor with I-BOP results in increased production of Aβ(1−40) by HEK293 cells coexpressing hAPP and hTP receptor. Aβ(1−40) levels in the media were measured by ELISA. (C) Increases in Aβ(1−40) release induced by treatment of HEK293 cells coexpressing hAPP and hTP with 0.8 nM I-BOP can be blocked by treatment with 10 μM of the known TP antagonists, daltroban and S18886. (D) TP receptor activation results in increased APP mRNA levels in HEK293 cells coexpressing hAPP and either hTP or mTP receptors. Cells were treated with 10 nM I-BOP in the absence or presence of 10 μM S18886, and APP mRNA levels were measured by qPCR and normalized to GAPDH mRNA. All values are presented as mean ± SD, ***$p < 0.001$ as determined by ANOVA and Tukey posthoc analysis.

coinciding with the appearance of Aβ plaque pathology.[18] Interestingly, iPF2αIII can bind to and activate the thromboxane A2-prostanoid (TP) receptor, a G-protein coupled receptor with two alternatively spliced isoforms (α and β) that demonstrate similar pharmacological properties.[19,20] The TP receptor is present on platelets and several other cell types, including neurons and glia within the mammalian brain,[20,21] and a recent study demonstrated that TP receptor activation by iPF2αIII elevates APP protein expression and consequently Aβ peptide levels through stabilization of APP mRNA.[22] These data thus suggest that formation of iPF2α during AD progression may further contribute to disease pathogenesis through pathways leading to increased Aβ deposition, and that inhibition of TP receptor activation by iPF2αIII may be an important unexplored therapeutic strategy to lower Aβ levels in AD. In support of this hypothesis are data which demonstrated that a TP antagonist, S18886,[23] could decrease plaque pathology and insoluble Aβ in the brains of Tg2576 mice.[22]

Although the normal function of the TP receptor in the brain is currently unknown, this receptor plays a pivotal role in regulating platelet aggregation and thus has been extensively studied as a drug target for controlling thrombosis.[24,25] We examined the BBB permeability of several representative examples of existing TP receptor antagonists, including S18886, to ascertain their potential to inhibit TP receptor activation in the brain, and found that all have poor brain penetration. The limited passage of these TP antagonists into the brain is likely due, at least in part, to the presence of a carboxylic acid moiety that may impede passive diffusion of the compound across the BBB,[26,27] thereby rendering the majority of known TP antagonists as suboptimal for the treatment of AD. In an attempt to identify BBB-permeable TP receptor antagonists, we have conducted a medicinal chemistry program that focused on the replacement of the carboxylic acid moiety of a S18886 congener, **5**,[23] with potential bioisosteres. To facilitate the characterization of these compounds, mouse TP (mTP) receptor and human TP (hTP) receptor cellular assays were developed. These include HEK293 cellular assays that permit the evaluation of compound effects on TP receptor-mediated changes in APP mRNA and protein levels, as well as Aβ peptide release, and TP receptor activity assays that measure receptor-mediated stimulation of intracellular inositol triphosphate (IP3) signaling. In addition, compounds were evaluated for brain penetration after administration to mice. Utilizing these tools, we have identified selected derivatives of **5** that
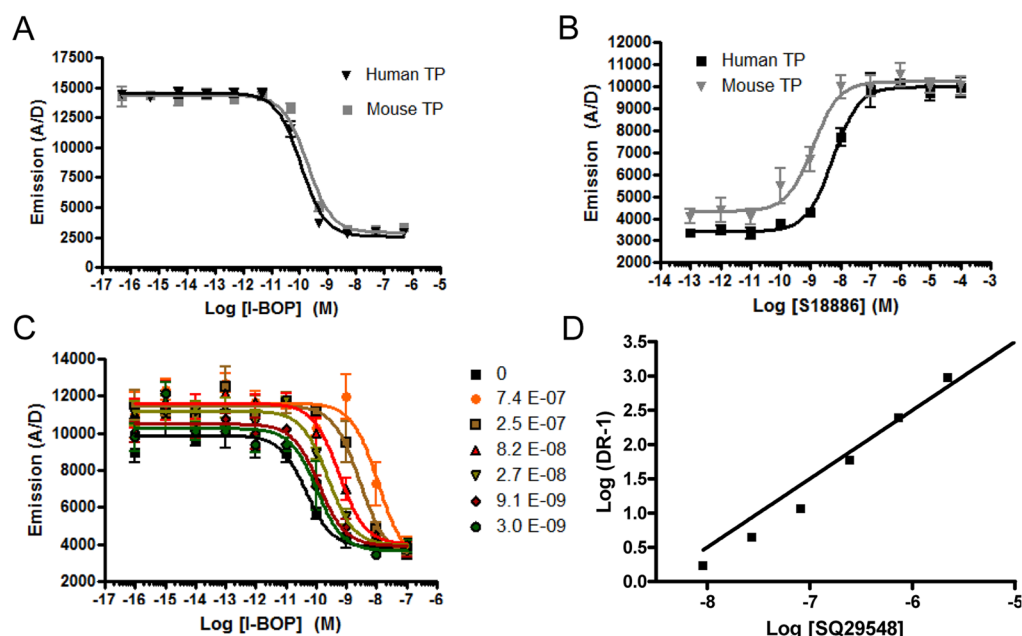
Figure 2. Analysis of TP receptor-mediated increases of IP1. (A) I-BOP binding to the hTP or mTP receptor results in increased production of IP1. HEK293 cells stably expressing the hTP receptor or mTP receptor were treated for 1 h with I-BOP at the indicated concentrations, and IP1 was measured as described in Methods. (B) The TP receptor antagonist, S18886, inhibits I-BOP-induced increases of IP1. HEK293 cells expressing the hTP or mTP receptors were incubated with varying concentrations of S18886 for 15 min, followed by the addition of 0.8 nM of I-BOP for 1 h. (C) I-BOP concentration−response curves were obtained at varying fixed concentrations of SQ25,548 (as shown in legend) by measuring IP1 formation in HEK293 cells expressing the mTP receptor. (D) Schild plot of the I-BOP concentration response curves from (C), with the x-intercept being equal to the K_d value. The K_d value derived from the mTP receptor Schild plot was 3.2 ± 1.4 nM, and a similar analysis for the hTP receptor yielded a K_d value of 6.9 ± 3.9 nM. All values represent mean ± SD.

freely enter the brain and retain moderately high affinity for both the mTP and hTP receptors.

■ RESULTS AND DISCUSSION

Previous data revealed that the TP receptor can regulate APP mRNA stability, and thus may play a role in AD pathogenesis.[22] To examine further the linkage between TP receptor activation and increased APP expression, we established HEK293 cell lines stably expressing human APP (hAPP) and the hTP receptor (α isoform). Treatment of these cells for 48 h with the potent TP agonist, [1S-1α,2β(5Z),3α(1E,3R*),4α]-7-[-3-(3-hydroxy-4-(4″-iodophenoxy)-1-butenyl)-7-oxabicyclo-[2.2.1]-heptan-2-yl]-5-heptenoic acid (I-BOP),[28] resulted in a dose-dependent increase in APP protein levels, with an EC_{50} of 0.8 nM as measured by immunoblot (Figure 1A). The I-BOP treatment also resulted in a 2.5-fold increase of Aβ(1−40) release from the hTP receptor-hAPP-expressing cells, as determined by ELISA, with an EC_{50} value of 0.3 nM (Figure 1B). A similar I-BOP-induced enhancement of Aβ(1−42) release was observed, although the absolute levels of Aβ(1−42) were lower than for Aβ(1−40) (not shown). To confirm that the I-BOP-induced effect on APP and Aβ levels is dependent on TP receptor activity, the hTP receptor-hAPP cells were concurrently treated with I-BOP and the known TP receptor antagonists, daltroban [29] or S18886 (structures shown in Table 1). Both antagonists decreased Aβ(1−40) release, with IC_{50} values of 105 and 16 nM for daltroban and S18886, respectively (Figure 1C).

To verify that the TP receptor-mediated effects on APP and Aβ levels resulted from changes in APP mRNA, quantitative PCR was performed on hTP receptor-hAPP cells treated with I-BOP. The I-BOP-treated cells showed a 3-fold increase in APP

mRNA (Figure 1D), which correlated well with the increase in APP protein and Aβ(1−40) production (Figure 1A and 1B). This I-BOP-induced increase of APP mRNA was blocked when the hTP receptor-hAPP cells were pretreated with S18886 (Figure 1D). HEK293 cells were also created that stably expressed the mTPα receptor and hAPP, and these cells showed a comparable increase of APP mRNA upon treatment with I-BOP that was inhibited by S18886 pretreatment (Figure 1D). These data thus confirm that TP receptor activation increases APP mRNA and protein expression, with a consequent elevation of Aβ(1−40/42) levels,[22] and these effects can be inhibited by known TP receptor antagonists.

The TP receptor-induced increase of APP mRNA is presumably mediated through the action of receptor-associated G-proteins, and it is known that the TP receptor couples primarily with G_q, although there is evidence of other G-protein subtype interactions.[30] To confirm that G_q is coupled to the hTP and mTP receptors in the HEK293 cells, a HTRF assay was utilized to measure the production of IP1, which is a metabolite of the IP3 that is formed after G_q-mediated phospholipase C activation. Treatment of cells expressing hTP or mTP receptors with I-BOP resulted in a dose-dependent increase in IP1 production, as evidenced by a decreased ratio of acceptor-to-donor fluorophore emission (A/D) following donor excitation in the HTRF assay, with EC_{50} values of 0.12 nM for hTP receptor cells and 0.19 nM for mTP receptor cells, respectively (Figure 2A). This assay thus provides a useful and robust method for measuring TP receptor activation. The TP receptor antagonist, S18886, blocked I-BOP-induced IP1 production, with an IC_{50} value of 5.4 nM in hTP receptor cells and 1.2 nM in mTP receptor cells (Figure 2B). We were also able to measure specific and

saturable binding of ^{3}H-SQ29,548, a radiolabeled TP receptor antagonist,[31,32] to membrane preparations from hTP or mTP receptor cells (not shown), with K_d values of 40 and 15 nM for the hTP and mTP receptors, respectively. However, the manufacture of ^{3}H-SQ29,548 was discontinued during the course of our studies, which led us to then approximate receptor binding affinities by the Schild method.[33,34] To validate the Schild method, I-BOP concentration−response curves were generated in the IP1 assay in the presence of increasing concentrations of SQ29,548, as depicted in Figure 2C for mTP receptor cells. A Schild plot of these data indicated an apparent K_d value of 3 nM for SQ29,548 interaction with the mTP receptor (Figure 2D), and a similar analysis of SQ29,548 with hTP receptor cells led to a calculated K_d value of 7 nM (not shown). These values are in general agreement with the binding affinities determined by radioligand binding, and suggest that the Schild method provides a reasonable approximation of receptor binding affinity.

The ability of known TP receptor antagonists to prevent agonist-induced increases of APP and Aβ suggests that such compounds may have utility in the treatment of AD. The vast majority of known TP receptor antagonists contain a carboxylic acid moiety, which is thought to be a critical contributor to the stability of the drug-receptor complex via ionic interaction with arginine residue 295 of the TP receptor.[35] However, this anionic group could hamper the passive diffusion of these compounds across the BBB.[26,36] We examined the brain penetration of several known TP receptor antagonists (see Table 1), with compounds administered (5 mg/kg i.p.) to wild-type mice, followed by mass spectrometric assessment of plasma and brain compound levels 1 h after dosing. There were very low to undetectable brain concentrations of all of the compounds, with brain-to-plasma (B/P) compound levels ≪ 1 (Table 1). Of the compounds tested, S18886 had the highest apparent brain penetration, with a B/P ratio of 0.14 that typically indicates poor BBB permeability. However, it is possible for a BBB-permeable compound to have a very low B/P ratio if the fraction of free, unbound compound is much greater in the brain than in the plasma (e.g., 7-fold greater unbound fraction in brain than plasma for a compound with a B/P ratio of 0.14). However, estimation of the unbound compound fraction in plasma (2.6%) and brain homogenate (4.4%) by a standard equilibrium dialysis methodology revealed only a 1.7-fold difference in free compound in these tissues, and thus S18886 does not appear to fully equilibrate across the BBB. The poor BBB permeability of existing TP receptor antagonists suggests that compounds that more readily enter the brain to modulate APP and Aβ levels would be desirable for the treatment of AD. Although a TP receptor antagonist with moderately low brain penetration, such as S18886, can reach sufficient brain concentrations to inhibit TP receptor activity when administered at relatively high doses to mice,[22] such doses result in very high plasma compound levels that could adversely affect platelet function when used chronically to treat elderly AD patients.

In an attempt to increase the B/P ratio of TP receptor antagonists, we investigated several analogues of the S18886-related tetrahydronaphthalene (THN), 5 (see Table 2), in which the carboxylic acid moiety was replaced by a range of heterocyclic bioisosteres, including the 1-H-tetrazole and nonacidic heterocycles, such as thiazoles or oxazoles. The syntheses of 5 and the corresponding tetrazole derivative 8 are highlighted in Scheme 1. In both cases, our synthesis entailed a

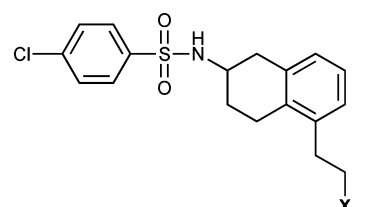**Table 1. Known TP Receptor Antagonists Are Poorly Brain-Penetrant**[a]

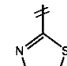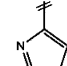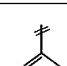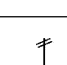| Compound	Structure	Brain (nM)	Plasma (nM)	B/P
Daltroban		<LOD	7226 (+/- 1009)	ND
S18886		187 (+/- 19)	1301 (+/- 431)	0.14
BM-567		46 (+/- 14)	5631 (+/- 803)	0.008
SQ29,548		<LOD	58 (+/- 20)	ND
Ramatroban		<LOD	920 (+/- 136)	ND
Vapiprost		8.1 (+/- 1.1)	654 (+/- 62)	0.012
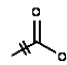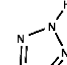
[a]1 month old mice were administered 5 mg/kg of antagonist. Drug levels were assessed by LC-MS/MS from brain and plasma samples obtained 1 h after dosing. LOD = below the limit of detection. ND = not determined. Values are presented as mean ± SD.

Heck coupling reaction to install the ethylacrylate onto the 5-bromo-2-tetralone (1)[37] to provide the keto-ester 2. Next, reductive amination of 2 with benzylamine was followed by catalytic hydrogenation and sulfonylation of the resulting amine to furnish ester 4, which could be hydrolyzed to 5, or used for the synthesis of 8. Thus, reduction of the ester moiety of 4 to alcohol 6 was followed by oxidative conversion of the primary alcohol to the nitrile 7,[38] which was finally reacted with sodium azide under microwave promoted conditions[39] to obtain the 1-H-tetrazole 8. The synthesis of oxazole and thiazole derivatives, illustrated in Scheme 2, started with the protection of ketone 1 as ketal, followed by a carbonylation reaction to obtain aldehyde 9. Next, Wittig olefination with the phosphonium salts of the appropriate heterocycles[40] furnished intermediates 10−13. Catalytic hydrogenation of the exocyclic double bond was then followed by TFA-mediated removal of the ketal (14−17). Finally, reductive amination of the ketone in the presence of ammonium trifluoroacetate and sodium triacetoxyborohydride generated the primary amine, which was directly used in the sulfonylation reaction to obtain the desired compounds (18−21).

All new compounds were evaluated for antagonist activity utilizing the IP1 assay with the hTP and mTP receptor-expressing cells, with the results summarized in Table 2. The

Table 2. Activities of Novel THN TP Receptor Antagonists As Assessed Using the IP1 Assay with Cells Expressing the hTP and mTP Receptors Stimulated with 0.2 nM I-BOP[a]

Compound	X	hIP1 IC$_{50}$ (nM)	mIP1 IC$_{50}$ (nM)
5		0.93 (+/- 0.50)	0.021 (+/- 0.021)
8		0.62 (+/- 0.45)	ND
18		347 (+/- 92.0)	87.5 (+/- 23.3)
19		370 (+/- 249)	118 (+/- 79.6)
20		512 (+/- 190)	92.2 (+/- 15.4)
21		1030 (+/- 365)	159 (+/- 71.8)

[a]Values are the means of at least three independent analyses, with associated SD. ND = not determined.

Scheme 2[a]
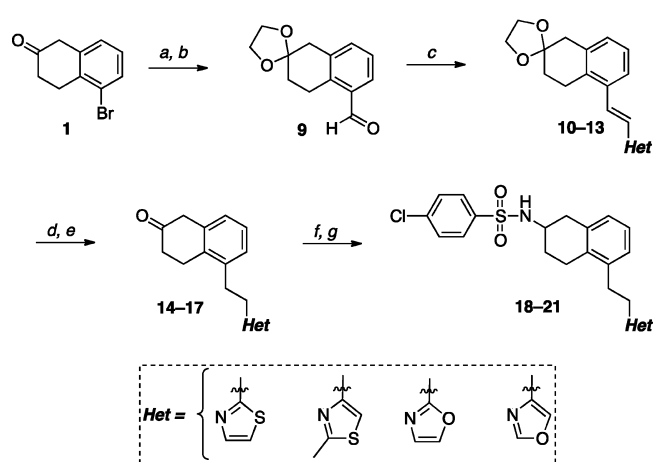
[a]Reagents and Reaction conditions: (a) ethylene glycol, PTSA, toluene, reflux, 16 h; (b) (i) *n*BuLi, −78 °C, THF, 30 min. (ii) *N,N*-DMF, THF, from −78 °C to −40 °C, 1 h; (c) appropriate tributylphosphonium chloride, potassium *tert*-butoxide, from −40 °C to rt, 1 h; (d) 1 atm of hydrogen, palladium on carbon, ethyl acetate/chloroform, 40 °C, 7 h; (e) TEA, DCM, 0°C to rt, 40 min.; (f) ammonium trifluoroacetate, sodium triacetoxyborohydride, rt, 5h; (g) 4-chlorophenylsulfonyl chloride, TEA, DCM, from 0 °C to rt, 16 h.

parent carboxylate-containing compound (**5**) was found to be an extremely potent TP receptor antagonist, which blocked I-BOP-induced IP1 production with an IC$_{50}$ of 0.93 (± 0.54) nM and 0.021 (± 0.021) nM using the hTP and mTP receptor-expressing cells. Like other anionic TP receptor antagonists, **5** did not efficiently cross the BBB, with a B/P ratio of 0.02 1 h after IP injection into mice (Table 3). Substitution of the carboxylic acid functionality of **5** with a tetrazole yielded a compound (**8**) with comparable antagonist activity to **5** in the hTP receptor-expressing cells (Table 2). However, like **5**, the tetrazole-containing analogue had poor BBB-permeability, with a B/P ratio of 0.01 (Table 3), and thus this compound did not undergo analysis in the mTP receptor assay. Replacing the

Scheme 1[a]
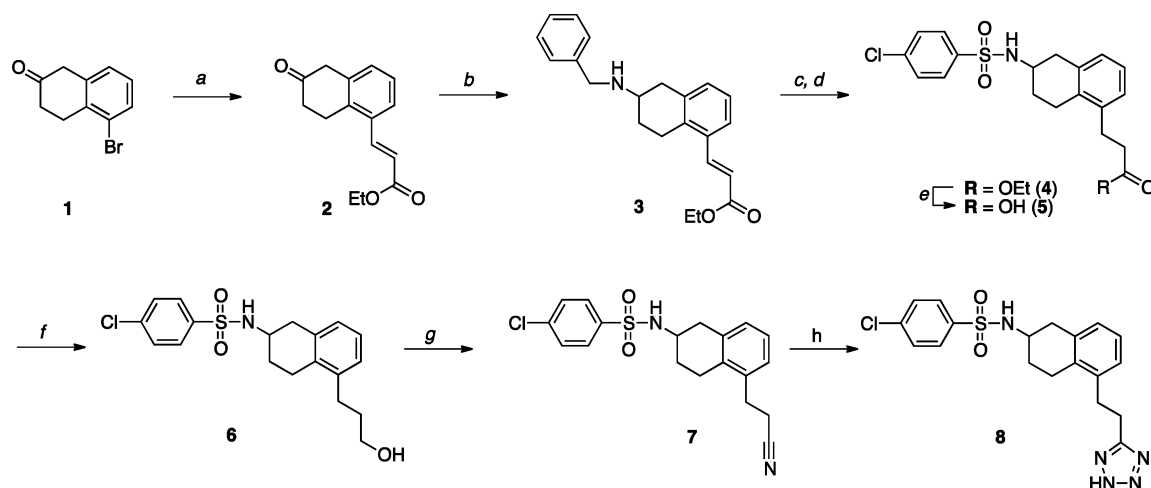
[a]Reagents and Reaction conditions: (a) ethyl acrylate, palladium(II) acetate, tri-*o*-tolylphosphine, TEA, 100 °C, 4 h; (b) (i) benzylamine, acetic acid, dichloroethane, rt, 45 min, (ii) sodium triacetoxyborohydride, rt, 16 h; (c) 1 atm of hydrogen, palladium on carbon, ethyl alcohol, 55 °C, 48 h; (d) 4-chlorophenylsulfonyl chloride, TEA, DCM, from 0°C to rt, 16 h; (e) sodium hydroxide, water/methanol, 55 °C, 1.5 h; (f) DIBAL-H, DCM −78 to 0 °C, 3 h; (g) ammonium hydroxide, iodine, 60°C, 24 h; (h) sodium azide, zinc bromide, 130 °C (microwave irradiation), 12 h.

Table 3. Evaluation of the Brain Penetration of Novel THN TP Receptor Antagonists[a]
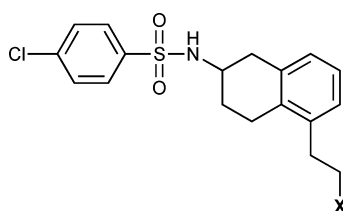
Compound	X	Plasma (nM)	Brain (nM)	B/P
5		10375.7 (+/- 3480.4)	212.9 (+/- 45.5)	0.022
8		865 (+/- 334)	8.3 (+/- 2.4)	0.012
18		163 (+/- 16)	198 (+/-17)	1.2
19		152 (+/- 57)	290 (+/- 141)	1.84
20		242 (+/- 34)	127 (+/- 16)	0.53
21		163 (+/- 34)	298 (+/- 33)	1.9

[a]Compounds were administered at 5 mg/kg to mice. Drug levels were assessed by LC-MS/MS from brain and plasma samples obtained 1 h after dosing. Values represent mean ± SD. B/P = brain/plasma ratio.

carboxylic acid moiety of **5** with nonacidic thiazoles (**18** and **19**) or oxazoles (**20** and **21**) resulted in analogues that blocked I-BOP-induced IP1 production in cells expressing the hTP and mTP receptors (Table 2), albeit with greater IC_{50} values than the very potent antagonist, **5**. However, as illustrated in Table 3, compounds **18−21** exhibited excellent brain penetration, with B/P ratios of at least 0.5 1 h after drug administration. A direct comparison of the activity of **20** and the prototype TP receptor antagonist, SQ29,548, in the IP1 assays revealed that both compounds had comparable IC_{50} values of 300−400 and 50−100 nM in cells expressing the hTP and mTP receptors, respectively (Figure 3A and Table 2). As SQ29,548 was demonstrated to have low nanomolar affinity for the TP receptors as measured by radioligand binding and Schild analyses (Figure 2), it appears that the IC_{50} values obtained in the IP1 functional assays underestimate receptor affinity, likely due to receptor reserve resulting from the high levels of receptor expression. Consequently, Schild analyses were performed with **20** to obtain a better approximation of receptor binding affinity. The results revealed apparent K_d values of 6 nM for the hTP receptor and 3 nM for the mTP receptor (Figure 3B), confirming that this compound binds with relatively high affinity at the TP receptors. Given that the thiazole and oxazole heterocyclic THN compounds displayed

similar IC_{50} values in the IP1 assays, it is likely that all of these brain-penetrant analogues interact at the hTP and mTP receptors with comparable affinity. The ability of these heterocyclic congeners of **5** to bind to the TP receptor with moderately high affinity is interesting, as the carboxylic acid moiety of TP receptor antagonists is thought to be a critical contributor to the stability of the drug−receptor complex via ionic interaction with arginine residue 295 of the TP receptor.[35] Although the carboxylic acid and tetrazole THN analogues clearly bind with greater affinity than **18−21**, the identification of reasonably potent TP receptor antagonists with excellent brain penetration indicates that these or related analogues may be further developed for central nervous system indications such as AD. To confirm that such compounds have an inhibitory effect on APP expression and Aβ release, cells expressing hAPP and the TP receptor were treated with I-BOP in the absence or presence of **19** or **20**. Both of these TP receptor antagonists significantly inhibited the I-BOP-induced increases of APP protein expression and Aβ(1−40) production by cells expressing the hTP (Figure 4A) or mTP (Figure 4B) receptors.

In summary, we have developed novel noncarboxylate TP receptor antagonists based on the THN scaffold found in previously described TP receptor antagonists.[41] Importantly, these compounds exhibit excellent brain penetration and reasonably high receptor binding affinity, and thus represent prototype brain-penetrant molecules designed to block TP receptor activation by iPF2αIII and/or thromboxane A2 in AD brain, with a resulting reduction of APP expression and Aβ release. The known TP receptor antagonist, S18886, was previously demonstrated to decrease Aβ plaque deposition in the Tg2576 mouse model of AD-like Aβ pathology when administered at 5 mg/kg/day for a 6 month period,[22] providing evidence that TP receptor antagonists may be plausible therapeutic interventions for AD. Sufficient brain concentrations of S18886 can be achieved at 5 mg/kg/day to inhibit TP receptor activity, but the relatively poor brain penetration of S18886 results in plasma concentrations that are 10-fold greater than in the brain. Although this did not prove to be problematic in the proof-of-concept study in Tg2576 mice, extremely high plasma levels of a TP receptor antagonist may not be well tolerated in older AD patients. The TP receptor is involved in platelet aggregation and prolonged receptor antagonism extends bleeding times in animals.[42,43] Moreover, humans with a gene defect in the TP receptor have an increased risk of bleeding.[44,45] Thus, we believe it is desirable to identify BBB-permeable TP receptor antagonists to minimize possible negative effects on hemostasis for indications where prolonged dosing would be required, such as AD. The vision is that a fully BBB-permeable TP receptor antagonist might achieve brain concentrations that result in reduced APP and Aβ levels, but have corresponding plasma compound levels that do not fully compromise platelet function.

■ METHODS

Compound Synthesis. All solvents were reagent grade. All reagents were purchased from Aldrich or Acros and used as received. Thin layer chromatography (TLC) was performed with 0.25 mm E. Merck precoated silica gel plates. Flash chromatography was performed with silica gel 60 (particle size 0.040−0.062 mm) supplied by Silicycle and Sorbent Technologies. Spots were detected by viewing under a UV light. Yields refer to chromatographically and spectroscopically pure compounds. Infrared spectra were recorded on a Jasco model FT/IR-480 Plus spectrometer. Proton (^{1}H) and
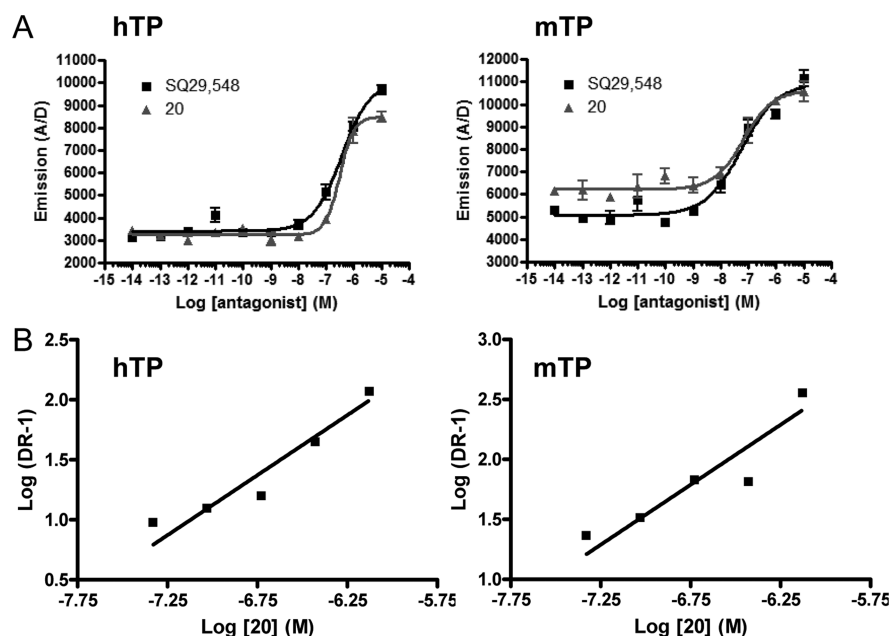
Figure 3. Comparison of SQ29,548 and compound **20** activities in the hTP and mTP receptor IP1 functional assay. (A) Cells expressing the hTP or mTP receptors were treated for 15 min with varying concentrations of SQ29,548 or **20**, followed by a 1 h treatment with 0.2 nM I-BOP before determining relative IP1 levels. The calculated IC_{50} values for SQ29,548 with the cells expressing the hTP and mTP receptor were 360 ± 140 and 55.6 ± 31.9 nM, respectively. The corresponding values for compound **20** were 307 ± 109 and 79.8 ± 58.2 nM. (B) Schild plots of compound **20** I-BOP concentration response curves in HEK293 cells stably expressing the hTP receptor (left) and mTP receptors (right). The K_d value derived from the hTP receptor Schild plot was 6.0 ± 2.9 nM, and a K_d value of 2.9 ± 1.2 nM was obtained from the mTP Schild plot. All data points represent mean ± SD.

carbon (^{13}C) NMR spectra were recorded on a Bruker AMX-500 spectrometer. Chemical shifts were reported relative to solvents. High-resolution mass spectra were measured at the University of Pennsylvania Mass Spectrometry Service on a Waters LCT Premier XE LC/MS system. Analytical reversed-phased (Sunfire C18; 4.6 × 50 mm, 5 mL) high-performance liquid chromatography (HPLC) was performed with a Water binary gradient module 2525 equipped with Waters 2996 PDA and Water micromass ZQ. All samples were analyzed employing a linear gradient from 10% to 90% of acetonitrile in water over 8 min and flow rate of 1 mL/min. Preparative reverse phase HPLC purification was performed on a Gilson HPLC system equipped with Gilson 333 pumps, a 215 Liquid Handler, 845Z injection module, and UV detector, employing Waters SunFire prep C18 OBD columns (5 μm 19 × 50 or 19 × 100 mm). All samples were purified employing a linear gradient from 10% to 90% of acetonitrile in water over 15 min and flow rate of 20 mL/min. Unless otherwise stated, all final compounds were found to be >95% as determined by HPLC/MS and NMR. All compounds were synthesized as racemic mixtures.

(E)-Ethyl-3-(6-oxo-5,6,7,8-tetrahydronaphthalen-1-yl)acrylate (2). A solution of 5-bromo-3,4-dihydronaphthalen-2(1H)-one (476.9 mg, 2.12 mmol), ethyl acrylate (0.28 mL, 2.58 mmol), palladium(II) acetate (4.8 mg, 0.02 mmol), and tri*o*-tolylphosphine (33.1 mg, 0.11 mmol) in triethylamine (2 mL) was heated at 100 °C in a sealed tube for 4 h. The reaction mixture was cooled to rt, diluted with dichloromethane (15 mL), and washed with hydrochloric acid (1 M, 10 mL). The organic layer was separated and the aqueous layer extracted with dichloromethane. The combined organic layers were dried over sodium sulfate and concentrated to dryness. Silica gel chromatography (20% ethyl acetate in hexanes) gave the purified product as yellow oil (385.6 mg). Yield: 74%. ^{1}H NMR (CDCl$_3$): δ 1.33 (t, J = 7.0 Hz, 3H), 2.52 (t, J = 6.5 Hz, 2H), 3.18 (t, J = 6.5 Hz, 2H), 3.58 (s, 2H), 4.26 (q, J = 7.0 Hz, 2H), 6.35 (d, J = 16.0 Hz, 1H), 7.13 (d, J = 7.5 Hz, 1H), 7.22 (t, J = 8.0 Hz, 1H), 7.46 (d, J = 7.5 Hz, 1H), 8.02 (d, J = 15.5 Hz, 1H) ppm.

(E)-Ethyl 3-(6-(benzylamino)-5,6,7,8-tetrahydronaphthalen-1-yl)-acrylate (3). A solution of (E)-ethyl-3-(6-oxo-5,6,7,8-tetrahydronaph-thalen-1-yl)acrylate (77 mg, 0.31 mmol) in dichloroethane (1.1 mL) was added with a solution of benzylamine (35 μL, 0.31 mmol) in dichloroethane (75 μL) followed by a second addition of acetic acid (71 μL, 1.3 mmol). The resulting mixture was stirred at rt for 45 min prior to an addition of sodium triacetoxyborohydride (375 mg, 1.7 mmol). The reaction mixture was allowed to stir at rt for 16 h, and then it was quenched by addition of saturated aqueous solution of sodium bicarbonate (2 mL). The pH was then adjusted to pH 8 by addition of sodium hydroxide (1 M solution in water), and the resulting mixture was extracted with dichloromethane; the organic layer dried over sodium sulfate and concentrated to dryness. The residue so obtained was finally purified by silica gel column chromatography (eluent: 10% methanol in dichloromethane) obtaining the title compound (93 mg, 0.28 mmol). Yield: 83%. ^{1}H NMR (CDCl$_3$): δ 1.34 (t, J = 7.0 Hz, 3H), 1.84–1.88 (m, 1H), 2.24–2.33 (m, 1H), 2.75–2.81 (m, 1H), 2.93–2.99 (m, 1H), 3.05–3.15 (m, 3H), 4.05 (broad s, 2H), 4.27 (q, J = 7.0 Hz, 2H), 6.32 (d, J = 15.5 Hz, 2H), 7.10–7.17 (m, 2H), 7.29–7.45 (m, 6H), 7.92 (d, J = 15.5 Hz, 1H) ppm. MS (ESI$^+$): calculated for C$_{22}$H$_{26}$NO$_2{}^+$, 336.2; found, 336.3.

Ethyl-3-(6-(4-chlorophenylsulfonamido)-5,6,7,8-tetrahydronaph-thalen-1-yl)propanoate (4). A solution of (E)-ethyl-3-(6-(benzylami-no)-5,6,7,8-tetrahydronaphthalen-1-yl)acrylate (120 mg, 0.36 mmol) in ethyl alcohol (10 mL) was added with hydrochloric acid (1.0 equiv, 1 N solution in water) followed by Pd on C (10 wt %; 50% wet). The resulting mixture was stirred under 1 atm of hydrogen for 48 h at 55 °C. The reaction mixture was then filtered through a Celite pad, and after evaporation of the volatiles the desired amine (100 mg, 0.35 mmol) was obtained as hydrochloride salt, which was redissolved in anhydrous dichloromehane (4 mL) and added at 5 °C with 4-chlorophenyl sulfonylchloride (75 mg, 0.35 mmol) followed by triethylamine (112 μL, 0.7 mmol). The resulting mixture was stirred for 3 h, allowing the temperature to rise to rt. The organic layer was then diluted with dichloromethane and extracted with water. The organic layer was then dried over sodium sulfate and concentrated to dryness. The residue so obtained was finally purified by column chromatography (silica gel; eluent, 30% ethyl actetate in hexanes) obtaining the title compound (85 mg, 0.20 mmol). Yield: 56%. ^{1}H
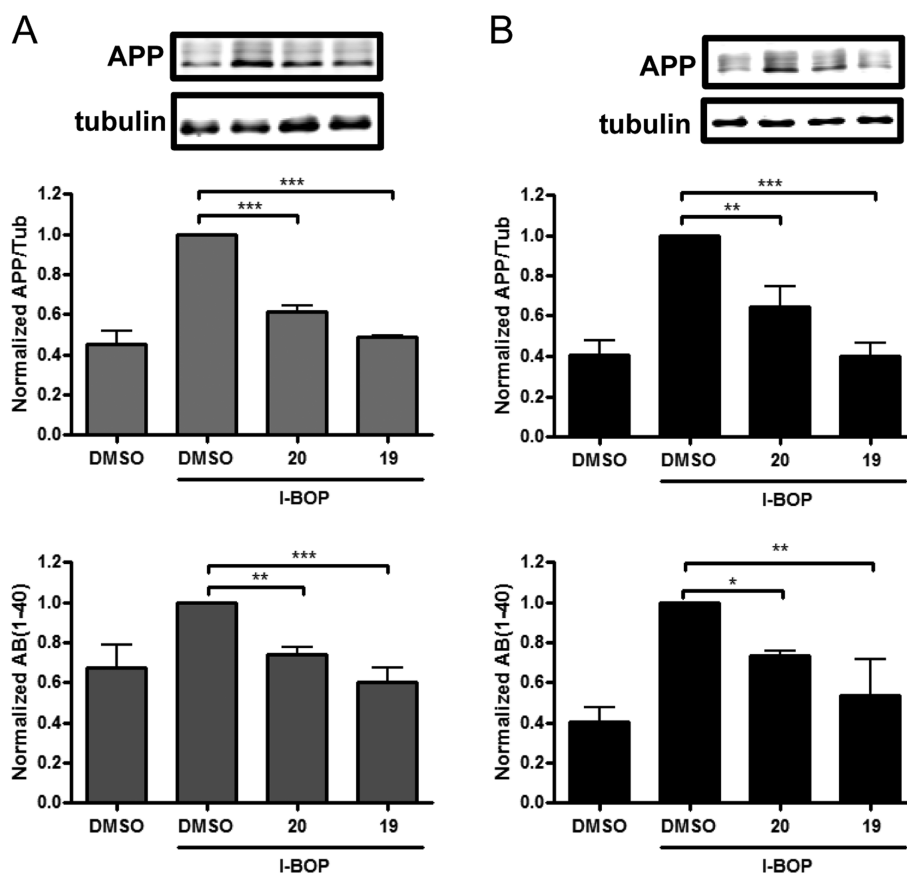
Figure 4. Compounds **19** and **20** reduce the I-BOP-induced APP protein expression and $A\beta(1-40)$ production by HEK293 cells expressing hTP receptor (A) or mTP receptor (B). Cells were pretreated for 1 h with either 10 μM **19** or **20**, or DMSO, followed by I-BOP (10 nM) for 48 h. Control cells did not receive test compound or I-BOP. APP levels were determined by immunoblotting and normalized to tubulin. $A\beta(1-40)$ was determined by ELISA measurement of culture medium. All values represent mean $\pm$ SD *$p < 0.05$, **$p < 0.01$, ***$p < 0.001$, as determined by ANOVA and Tukey posthoc analysis.

NMR (CDCl$_3$): δ 1.26 (t, $J = 7.0$ Hz, 3H), 1.77 (m, 1H), 1.96–2.0 (m, 1H), 2.53–2.56 (m, 2H), 2.62–2.71 (m, 2H), 2.71–2.87 (m, 3H), 2.94 (dd, $J = 16.0/5.0$ Hz, 1H), 3.63 (m, 1H), 4.14 (q, $J = 7.0$ Hz, 2H), 5.04 (d, $J = 7.5$ Hz, 1H), 6.83 (d, $J = 7.5$ Hz, 1H), 7.00 (d, $J = 7.0$ Hz, 1H), 7.06 (t, $J = 7.5$ Hz, 1H), 7.49 (d, $J = 9.0$ Hz, 2H), 7.83 (d, $J = 9.0$ Hz, 2H) ppm. ^{13}C NMR (CDCl$_3$): 14.4, 24.0, 27.8, 29.6, 34.5, 37.1, 49.3, 60.7, 126.3, 126.8, 128.0, 128.6, 129.6, 133.2, 133.7, 138.8, 139.2, 139.7, 173.1 ppm. MS (ESI$^+$): calculated for C$_{21}$H$_{25}$ClNO$_4$S$^+$, 422.1; found, 422.1.

3-(6-(4-Chlorophenylsulfonamido)-5,6,7,8-tetrahydronaphthalen-1-yl)propanoic acid (5). A solution of ethyl-3-(6-(4-chlorophenylsulfonamido)-5,6,7,8-tetrahydronaphthalen-1-yl)propanoate (23 mg, 0.05 mmol) in a mixture containing methanol (1 mL) and water (1 mL) was added with sodium hydroxide (220 μL of a 1 M solution in water, 0.22 mmol). The resulting mixture was then stirred at 55 °C for 1.5 h. The pH of the reaction mixture was then adjusted to pH 5.5 by addition of a 1 N aqueous solution of hydrochloric acid, and the resulting mixture was extracted with ethyl acetate. The organic layer was then dried over sodium sulfate and concentrated to dryness obtaining the title compound (19 mg). Yield: 91%. ^{1}H NMR (CD$_3$OD): δ 1.68–1.72 (m, 1H), 1.93–1.96 (m, 1H), 2.50–2.53 (m, 2H), 2.61–2.68 (m, 2H), 2.81–2.86 (m, 4H), 3.46–3.51 (m, 1H), 6.73 (d, $J = 6.5$ Hz, 1H), 6.96–7.00 (m, 2H), 7.57 (d, $J = 9.0$ Hz, 2H), 7.87 (d, $J = 9.0$ Hz, 2H) ppm. ^{13}C NMR (CD$_3$OD): 25.6, 28.9, 31.1, 35.3, 38.0, 50.9, 127.1, 127.5, 128.7, 129.7, 130.5, 134.5, 135.6, 139.8, 139.9, 142.2, 176.9 ppm. MS (ESI$^+$): calculated for C$_{19}$H$_{21}$ClNO$_4$S$^+$, 394.1; found, 394.3.

4-Chloro-N-(5-(3-hydroxypropyl)-1,2,3,4-tetrahydronaphthalen-2-yl)benzenesulfonamide (6). Diisobutylaluminium hydride in dichloromethane (0.84 mL, 1 M, 0.84 mmol) was added dropwise

to a solution of ethyl-3-(6-(4-chlorophenylsulfonamido)-5,6,7,8-tetrahydronaphthalen-1-yl)propanoate (60 mg, 0.14 mmol) in dichloromethane (2 mL) at −78 °C. The reaction was allowed to warm to 0 °C over 3 h. Sodium potassium tartrate solution (10 mL, 1 M aqueous solution) was then added, and stirring continued at rt for 1 h. The organic layer was separated, and the aqueous layer extracted with dichloromethane. The combined organic layers were dried over sodium sulfate and concentrated to dryness. Silica gel chromatography (50% ethyl acetate in hexanes) gave the purified product as colorless oil (54 mg). Yield: 100%. ^{1}H NMR (CDCl$_3$): δ 1.74–1.84 (m, 3H), 1.96–2.00 (m, 1H), 2.59–2.65 (m, 3H), 2.68–2.72 (m, 1H), 2.73–2.85 (m, 1H), 2.93–2.97 (m, 1H), 3.66 (m, 1H), 3.71 (t, $J = 12.5$ Hz, 2H), 4.82 (bs, 1H), 6.82 (d, $J = 7.5$ Hz, 1H), 7.01–7.03 (m, 1H), 7.05–7.08 (m, 1H), 7.47 (d, $J = 9.0$ Hz, 2H), 7.83 (d, $J = 9.0$ Hz, 2H) ppm. ^{13}C NMR (CDCl$_3$): 23.8, 29.0, 29.7, 32.9, 37.1, 49.3, 62.6, 126.3, 127.2, 127.7, 128.6, 129.6, 133.1, 133.5, 139.2, 139.7, 140.2 ppm. IR: ν 3505, 3276, 2934, 2878, 1585 cm^{-1}. HRMS (ESI$^-$): calculated for C$_{19}$H$_{21}$ClNO$_3$S$^-$, 378.0931; found, 378.0915.

4-Chloro-N-(5-(2-cyanoethyl)-1,2,3,4-tetrahydronaphthalen-2-yl)benzenesulfonamide (7). A solution of 4-chloro-N-(5-(3-hydroxypropyl)-1,2,3,4-tetrahydronaphthalen-2-yl)benzene-sulfonamide (55 mg, 0.14 mmol) in ammonium hydroxide (1.5 mL) was added with iodine (110 mg, 0.43 mmol), and the resulting mixture was stirred at 60 °C for 24 h. The reaction was then quenched at 0 °C by addition of a saturated solution of sodium sulfite (2 mL). The mixture so obtained was extracted with dichloromethane. The organic layer was then dried over magnesium sulfate and concentrated to dryness; the resulting material was purified by column chromatography (silica gel; Biotage SP4; gradient of ethyl acetate in hexanes) obtaining the title compound (15.7 mg). Yield: 29%. ^{1}H NMR (CDCl$_3$): δ 1.79–1.82

(m, 1H), 1.99–2.02 (m, 1H), 2.58 (t, J = 7.5 Hz, 2H), 2.63–2.73 (m, 2H), 2.79–2.84 (m, 1H), 2.91 (t, J = 7.5 Hz, 2H), 2.95–2.99 (m, 1H), 3.64–3.69 (m, 1H), 4.83 (d, J = 7.6 Hz, 1H), 4.98 (bs, 1H), 6.90 (d, J = 7.6 Hz, 1H), 7.04 (d, J = 7.5 Hz, 1H), 7.11 (t, J = 7.5 Hz, 1H), 7.50 (d, J = 9.0 Hz, 2H), 7.83 (d, J = 9.0 Hz, 2H) ppm. ^{13}C NMR (CDCl$_3$): 18.0, 23.9, 28.2, 29.5, 37.0, 49.1, 119.2, 126.2, 127.1, 128.1, 128.6, 129.0, 129.6, 133.0, 134.1, 136.3, 139.3 ppm. IR: ν 3268, 2931, 2248, 1586 cm^{-1}. HRMS (ESI$^+$): calculated for C$_{19}$H$_{19}$ClN$_2$O$_2$SNa$^+$, 397.0753; found, 397.0760.

N-(5-(2-(2H-Tetrazol-5-yl)ethyl)-1,2,3,4-tetrahydronaphthalen-2-yl)-4-chlorobenzenesulfonamide (8). 4-Chloro-*N*-(5-(2-cyanoethyl)-1,2,3,4-tetrahydronaphthalen-2-yl)benzenesulfonamide (126 mg, 0.37 mmol) was added with a 1 M aqueous solution of sodium azide (367 μL, 0.37 mmol) and a 1 M aqueous solution of zinc bromide (335 μL, 0.33 mmol). The resulting mixture was stirred in a microwave reactor at 130 °C for 12 h. The reaction vial was then repeatedly washed with 1 N hydrochloric acid and ethyl acetate until no solid residues were observed. The water layer was extracted with ethyl acetate, and the combined organic extracts were then dried over magnesium sulfate and evaporated to dryness. The residue obtained was finally purified by column chromatography (silica gel; Biotage SP4; gradient of methanol in dichloromethane) obtaining the title compound (20.0 mg). Yield: 14%. ^{1}H NMR (MeOD): δ 1.71–1.77 (m, 1H), 1.96–2.00 (m, 1H), 2.71 (m, 2H), 2.90 (d, J = 16.8 Hz, 2H), 3.05 (t, J = 7.8 Hz, 2H), 3.18–3.22 (m, 2H), 3.51–3.55 (m, 1H), 6.85 (d, J = 7.6 Hz, 1H), 6.90 (d, J = 7.4 Hz, 1H), 7.01 (t, J = 7.6 Hz, 1H), 7.62 (d, J = 8.8 Hz, 2H), 7.91 (d, J = 8.8 Hz, 2H). ^{13}C NMR (MeOD): 24.9, 25.6, 31.1, 31.7, 38.0, 50.9, 127.3, 127.9, 129.2, 129.8, 130.6, 134.7, 136.0, 138.9, 139.8, 142.3, 157.6 ppm. IR: ν 3268, 2920, 2848, 1707, 1586 cm^{-1}. HRMS (ESI$^-$): calculated for C$_{19}$H$_{19}$ClN$_5$O$_2$S$^-$, 416.0936; found, 416.0948.

3′,4′-Dihydro-1′H-spiro[[1,3]dioxolane-2,2′-naphthalene]-5′-carbaldehyde (9). A solution of 5-bromo-3,4-dihydronaphthalen-2(1H)-one (625 mg, 2.78 mmol), ethylene glycol (0.23 mL, 4.17 mmol), and *p*-toluenesulfonic acid (5.70 mg, 0.03 mol) in benzene (46 mL) was stirred and heated to reflux for 10 h. The solution was cooled, diluted with ether, and sequentially washed with saturated aqueous sodium bicarbonate solution and water. The organic layer was dried over magnesium sulfate, filtered and concentrated in vacuo. Purification by silica gel column chromatography, using a 2:1 mixture of hexanes and AcOEt as eluant, furnished 5′-bromo-3′,4′-dihydro-1′H-spiro[[1,3]-dioxolane-2,2′-naphthalene] (730.4 mg, 98% yield) as a yellow oil. Yield: 65%. ^{1}H NMR (500 MHz; CDCl$_3$): δ 1.98 (t, J = 6.9 Hz, 2H), 3.00 (d, J = 6.4 Hz, 4H), 4.03 (s, 4H), 6.97–7.01 (m, 2H), 7.40 (dd, J = 7.1, 1.9 Hz, 1H) ppm. ^{13}C NMR (126 MHz; CDCl$_3$): δ 29.3, 31.6, 39.3, 64.6, 107.8, 125.2, 127.2, 128.5, 130.3, 134.9, 136.8 ppm. To a solution of 5′-bromo-3′,4′-dihydro-1′H-spiro[[1,3]dioxolane-2,2′-naphthalene] (2.01 g, 7.47 mmol) in anhydrous tetrahydrofuran (74 mL) was added *n*-BuLi (2.50 M in hexane, 4.48 mL, 11.2 mmol) at −78 °C under nitrogen atmosphere. The mixture was stirred for 10 min at −78 °C under nitrogen atmosphere and then added with anhydrous *N,N*-dimethylformamide (0.86 mL, 11.2 mmol) in anhydrous tetrahydrofuran (1 mL) at −78 °C. The reaction mixture was stirred for 1 h, allowing the temperature to rise to −40 °C, and then it was quenched by addition of saturated aqueous ammonium chloride solution. The mixture was extracted with ethyl acetate. The combined organic layers were washed with brine, dried over magnesium sulfate, filtered, and concentrated in vacuo. Purification by silica gel column chromatography, using a 5:1 mixture of hexanes/ethyl acetate as eluant, furnished the desired aldehyde (1.23 g, 75%) as a colorless oil. ^{1}H NMR (500 MHz; CDCl$_3$): δ 1.99 (t, J = 6.8 Hz, 2H), 3.05 (s, 2H), 3.44 (t, J = 6.8 Hz, 2H), 4.04 (s, 4H), 7.29–7.34 (m, 2H), 7.66 (dd, J = 7.1, 1.7 Hz, 1H), 10.24 (s, 1H) ppm. ^{13}C NMR (126 MHz; CDCl$_3$): δ 25.3, 31.1, 39.5, 64.6, 107.2, 126.2, 131.6, 133.8, 135.1, 136.5, 137.8, 193.0 ppm.

General Procedure for the Synthesis of 10–13. To a suspension of the appropriate phosphonium chloride (0.25 mmol) in anhydrous tetrahydrofuran (1.0 mL) was added potassium *tert*-butoxide (1.0 M in tetrahydrofuran, 0.44 mL, 0.44 mmol) at 0 °C. The mixture was stirred for 10 min at 0 °C and then cooled to −40 °C. To this stirring mixture, a solution of the 3′,4′-dihydro-1′H-spiro[[1,3]dioxolane-2,2′-

naphthalene]-5′-carbaldehyde (50 mg, 0.23 mmol) in anhydrous tetrahydrofuran (1.3 mL) was added dropwise. The reaction mixture was stirred for 40 min while allowing the temperature to gradually rise to room temperature. The reaction mixture was quenched by addition of saturated aqueous ammonium chloride solution and extracted with ether. The organic layer was washed with saturated aqueous ammonium chloride solution, dried over magnesium sulfate, filtered, and concentrated in vacuo. Purification by silica gel column chromatography, using a 2:1 mixture of hexanes/AcOEt as eluant, furnished the desired compound.

(E)-2-(2-(3′,4′-Dihydro-1′H-spiro[[1,3]dioxolane-2,2′-naphthalen]-5′-yl)vinyl)thiazole (10). Yield: 95%. ^{1}H NMR (500 MHz; CDCl$_3$): δ 1.54 (s, 2H), 2.01 (t, J = 6.8 Hz, 2H), 3.02 (s, 2H), 3.10 (t, J = 6.8 Hz, 2H), 4.03–4.05 (m, 4H), 7.05 (d, J = 7.6 Hz, 1H), 7.15–7.19 (m, 2H), 7.25 (d, J = 3.3 Hz, 1H), 7.45 (d, J = 7.7 Hz, 1H), 7.70 (d, J = 16.0 Hz, 1H), 7.80 (d, J = 3.3 Hz, 1H) ppm.

(E)-4-(2-(3′,4′-Dihydro-1′H-spiro[[1,3]dioxolane-2,2′-naphthalen]-5′-yl)vinyl)-2-methylthiazole (11). Yield: 93%. ^{1}H NMR (500 MHz; CDCl$_3$): δ 2.00 (t, J = 6.8 Hz, 2H), 2.74 (s, 3H), 3.02 (s, 2H), 3.11 (t, J = 6.8 Hz, 2H), 4.03 (d, J = 2.1 Hz, 4H), 6.90 (d, J = 15.7 Hz, 1H), 6.99 (d, J = 9.9 Hz, 2H), 7.14 (t, J = 7.6 Hz, 1H), 7.40 (d, J = 7.7 Hz, 1H), 7.66 (d, J = 15.7 Hz, 1H) ppm.

(E)-2-(2-(3′,4′-Dihydro-1′H-spiro[[1,3]dioxolane-2,2′-naphthalen]-5′-yl)vinyl)oxazole (12). Yield: 78%. ^{1}H NMR (500 MHz; CDCl$_3$): δ 2.00 (t, J = 6.8 Hz, 2H), 3.02 (s, 2H), 3.09 (t, J = 6.8 Hz, 2H), 4.03 (d, J = 1.3 Hz, 4H), 6.84 (d, J = 16.2 Hz, 1H), 7.05 (d, J = 7.6 Hz, 1H), 7.15–7.18 (m, 2H), 7.43 (d, J = 7.4 Hz, 1H), 7.62 (s, 1H), 7.77 (d, J = 16.2 Hz, 1H) ppm. ^{13}C NMR (126 MHz; CDCl$_3$): δ 25.7, 31.5, 39.5, 64.58, 107.7, 115.5, 123.9, 126.3, 128.5, 130.4, 133.8, 134.4, 135.3, 138.1, 161.9 ppm.

(E)-4-(2-(3′,4′-Dihydro-1′H-spiro[[1,3]dioxolane-2,2′-naphthalen]-5′-yl)vinyl)oxazole (13). Yield: 94%. ^{1}H NMR (500 MHz; CDCl$_3$): δ 1.99 (t, J = 6.8 Hz, 2H), 3.01 (s, 2H), 3.09 (t, J = 6.8 Hz, 2H), 4.03 (d, J = 1.3 Hz, 4H), 6.79 (d, J = 15.8 Hz, 1H), 7.00 (d, J = 7.6 Hz, 1H), 7.14 (t, J = 7.6 Hz, 1H), 7.39 (d, J = 7.7 Hz, 1H), 7.58 (d, J = 15.8 Hz, 1H), 7.65 (s, 1H), 7.87 (d, J = 0.5 Hz, 1H) ppm.

General Procedure for the Synthesis of 14–17. A mixture containing the appropriate olefin (0.39 mmol), 10% Pd/C(40 mg), ethyl acetate (25 mL), and chloroform (1 mL) was stirred under hydrogen atmosphere at 40 °C for 7 h and then filtered through a pad of Celite. The filtered solution was then evaporated to dryness, obtaining the saturated intermediate in >95% yield, which was used directly for the next step. Thus, trifluoroacetic acid (0.5 mL) was added dropwise to solution of the appropriate ketal (0.35 mmol) in dichloromethane (3 mL) at 0 °C. The reaction mixture was then stirred for 40 min, allowing the temperature to rise to room temperature. The reaction was quenched by addition of saturated aqueous solution of sodium bicarbonate at 0 °C, and the resulting mixture was extracted with dichloromethane. The combined organic layers were washed with saturated aqueous solution of sodium bicarbonate, dried over magnesium sulfate, and concentrated in vacuo. Purification by silica gel column chromatography, using a 2:1 mixture of hexanes/AcOEt as eluant, furnished the desired compound.

5-(2-(Thiazol-2-yl)ethyl)-3,4-dihydronaphthalen-2(1H)-one (14). Yield: 62%. ^{1}H NMR (500 MHz; CDCl$_3$): δ 2.48 (t, J = 6.6 Hz, 2H), 3.06 (t, J = 6.6 Hz, 2H), 3.20 (m, 2H), 3.30–3.27 (m, 2H), 3.59 (s, 2H), 7.01 (d, J = 7.2 Hz, 1H), 7.15 (dt, J = 14.2, 7.1 Hz, 2H), 7.20 (d, J = 3.3 Hz, 1H), 7.71 (d, J = 3.3 Hz, 1H) ppm.

5-(2-(2-Methylthiazol-4-yl)ethyl)-3,4-dihydronaphthalen-2(1H)-one (15). Yield: 31%. ^{1}H NMR (500 MHz; CDCl$_3$): δ 2.45 (t, J = 6.6 Hz, 2H), 2.71 (s, 3H), 2.97 (dd, J = 9.4, 6.3 Hz, 2H), 3.09–3.02 (m, 4H), 3.57 (s, 2H), 6.64 (s, 1H), 6.99 (d, J = 7.2 Hz, 1H), 7.13 (m, 2H) ppm.

5-(2-(Oxazol-2-yl)ethyl)-3,4-dihydronaphthalen-2(1H)-one (16). Yield: 71%. ^{1}H NMR (500 MHz; CDCl$_3$): 2.51 (t, J = 6.6 Hz, 2H), 3.08–3.02 (m, 4H), 3.16 (dd, J = 9.2, 6.7 Hz, 2H), 3.58 (s, 2H), 7.03–7.00 (m, 2H), 7.10 (d, J = 6.8 Hz, 1H), 7.15 (t, J = 7.5 Hz, 1H), 7.57 (d, J = 0.8 Hz, 1H) ppm. ^{13}C NMR (126 MHz; CDCl$_3$): δ 24.1, 29.4, 30.5, 37.9, 45.7, 126.92, 126.99, 127.03, 127.7, 134.0, 135.0, 137.4, 138.4, 163.9, 210.6 ppm.

5-(2-(Oxazol-4-yl)ethyl)-3,4-dihydronaphthalen-2(1H)-one **(17)**. Yield: 50%. ^{1}H NMR (500 MHz; CDCl$_3$): δ 2.48 (t, *J* = 6.6 Hz, 2H), 2.81 (t, *J* = 7.9 Hz, 2H), 3.07−3.02 (m, 4H), 3.58 (s, 2H), 7.00 (d, *J* = 7.3 Hz, 1H), 7.09 (d, *J* = 7.2 Hz, 1H), 7.14 (d, *J* = 7.5 Hz, 1H), 7.88 (s, 1H), 7.36 (s, 1H) ppm. ^{13}C NMR (126 MHz; CDCl$_3$): δ 24.1, 27.5, 32.0, 37.9, 45.7, 126.6, 126.8, 127.9, 133.8, 134.6, 135.1, 138.2, 139.4, 151.1, 210.8 ppm.

General Procedure for the Synthesis of 18−21. A solution of the appropriate ketone (0.19 mmol) and ammomium trifluoroacetate (50 mg, 0.23 mmol) in tetrahydrofuran (0.3 mL) was stirred for 20 min at room temperature. The reaction mixture was then added with sodium triacetoxyborohydride (50 mg, 0.23 mmol) and stirred at room temperature for 5 h. The reaction was then quenched by addition of 1 mL of concentrated hydrochloric acid. The reaction mixture was vigorously stirred for 15 min and then diluted with water (8 mL) and extracted with ether. The combined organic layers were dried over magnesium sulfate, filtered, and concentrated in vacuo to give the amine intermediate, which was used directly for the next step. Thus, to a solution of the appropriate amine (0.068 mmol) in 0.7 mL of dry dichloromethane and triethylamine (10 μL, 0.07 mmol) was added 4-chlorobenzenesulfonyl chloride (15 mg, 0.07 mmol) with stirring at 0 °C. The reaction mixture was stirred for 16 h, allowing the temperature to rise to room temperature. The reaction was quenched by addition of saturated aqueous solution of ammonium chloride. The resulting mixture was extracted with dichloromethane. The combined organic layers were washed with saturated aqueous solution of ammonium chloride, dried over magnesium sulfate, and concentrated in vacuo. Purification by silica gel preparative TLC using a 2:1 mixture of hexane/AcOEt as eluent furnished the desired compound.

4-Chloro-N-(5-(2-(thiazol-2-yl)ethyl)-1,2,3,4-tetrahydronaphthalen-2-yl)benzenesulfonamide **(18)**. Yield: 18% over two steps. ^{1}H NMR (500 MHz; CDCl$_3$): δ 1.81−1.73 (m, 1H), 1.96 (m, 1H), 2.63 (dd, *J* = 16.2, 7.5 Hz, 1H), 2.75 (m, 2H), 2.97 (dd, *J* = 16.2, 4.7 Hz, 1H), 3.06−3.03 (m, 2H), 3.32−3.21 (m, 2H), 3.71−3.66 (m, 1H), 4.62 (d, *J* = 7.9 Hz, 1H), 6.84 (d, *J* = 7.4 Hz, 1H), 7.05 (m, 2H), 7.21 (d, *J* = 3.3 Hz, 1H), 7.49 (d, *J* = 8.7 Hz, 2H), 7.70 (d, *J* = 3.3 Hz, 1H), 7.82 (d, *J* = 8.7 Hz, 2H) ppm. ^{13}C NMR (126 MHz; CDCl$_3$): δ 23.9, 29.6, 33.0, 33.7, 37.1, 49.2, 118.6, 126.5, 127.3, 128.6, 128.2, 129.7, 133.3, 133.6, 138.7, 139.3, 139.7, 142.5, 170.2 ppm. IR: ν 3276, 3085, 2930, 1581 cm^{-1}. HRMS: calculated for C$_{21}$H$_{22}$N$_2$O$_2$S$_2$Cl$^+$, 433.0811; found, 433.0800

4-Chloro-N-(5-(2-(2-methylthiazol-4-yl)ethyl)-1,2,3,4-tetrahydronaphthalen-2-yl)benzenesulfonamide **(19)**. Yield: 42% over two steps. ^{1}H NMR (500 MHz; CDCl$_3$): δ 1.80−1.73 (m, 1H), 1.97 (m, 1H), 2.63 (dd, *J* = 16.2, 7.7 Hz, 1H), 2.71 (dd, *J* = 24.4, 7.1 Hz, 4H), 2.81 (dq, *J* = 15.9, 5.0 Hz, 1H), 2.98−2.90 (m, 5H), 3.67 (m, 1H), 4.61 (d, *J* = 7.8 Hz, 1H), 6.66 (s, 1H), 6.82 (d, *J* = 7.2 Hz, 1H), 7.04 (m Hz, 2H), 7.49 (d, *J* = 8.6 Hz, 2H), 7.82 (d, *J* = 8.6 Hz, 2H) ppm. ^{13}C NMR (126 MHz; CDCl$_3$): δ 19.2, 23.7, 29.6, 31.9, 32.3, 37.0, 49.2, 112.7, 126.2, 127.1, 127.6, 128.5, 129.4, 133.04, 133.20, 139.1, 139.69, 139.71, 156.1, 165.6 ppm. IR: ν 3281, 2925, 1588 cm^{-1}. HRMS: calculated for C$_{22}$H$_{24}$N$_2$O$_2$S$_2$Cl$^+$, 447.0068; found, 447.0963.

4-Chloro-N-(5-(2-(oxazol-2-yl)ethyl)-1,2,3,4-tetrahydronaphthalen-2-yl)benzenesulfonamide **(20)**. Yield: 23% over two steps. ^{1}H NMR (500 MHz; CDCl$_3$): δ 1.84−1.76 (m, 1H), 2.02−1.96 (m, 1H), 2.64 (dd, *J* = 16.2, 7.6 Hz, 1H), 2.77−2.72 (m, 1H), 2.82 (dd, *J* = 15.0, 8.7 Hz, 1H), 3.01−2.95 (m, 1H), 3.04−3.03 (m, 3H), 3.70 (m, 1H), 4.66 (d, *J* = 7.9 Hz, 1H), 6.86 (d, *J* = 7.4 Hz, 1H), 7.05 (m, 3H), 7.51 (d, *J* = 8.7 Hz, 2H), 7.58 (d, *J* = 0.8 Hz, 1H), 7.84 (d, *J* = 8.7 Hz, 2H) ppm. ^{13}C NMR (126 MHz; CDCl$_3$): δ 23.6, 28.4, 29.5, 29.8, 37.0, 49.1, 126.3, 126.87, 127.00, 128.1, 128.4, 129.5, 133.0, 133.4, 138.38, 138.47, 139.1, 139.7, 164.1 ppm. IR: ν 3274, 2926, 1576 cm^{-1}. HRMS: calculated for C$_{21}$H$_{22}$N$_2$O$_3$SCl$^+$, 417.1040; found, 417.1031.

4-Chloro-N-(5-(2-(oxazol-4-yl)ethyl)-1,2,3,4-tetrahydronaphthalen-2-yl)benzenesulfonamide **(21)**. Yield: 29% over two steps. ^{1}H NMR (500 MHz; CDCl$_3$): δ 1.81−1.74 (m, 1H), 2.00−1.95 (m, 1H), 2.62 (dd, *J* = 16.2, 7.5 Hz, 1H), 2.83−2.69 (m, 4H), 2.90−2.85 (m, 2H), 3.01−2.94 (m, 1H), 3.69 (m, 1H), 4.58 (d, *J* = 7.9 Hz, 1H), 6.83 (d, *J* = 7.5 Hz, 1H), 7.01 (d, *J* = 6.8 Hz, 1H), 7.06 (t, *J* = 7.5 Hz, 1H), 7.37 (d, *J* = 0.9 Hz, 1H), 7.49 (d, *J* = 8.6 Hz, 2H), 7.84−7.81 (m, 3H)

ppm. ^{13}C NMR (126 MHz; CDCl$_3$): δ 23.7, 26.5, 29.5, 31.4, 37.0, 49.2, 126.2, 127.1, 127.8, 128.4, 129.4, 133.0, 133.3, 134.4, 139.1, 139.4, 139.7, 151.0 ppm. IR: ν 3277, 2926, 1588 cm^{-1}. HRMS: calculated for C$_{21}$H$_{21}$N$_2$O$_3$NaSCl$^+$, 439.0859; found, 439.0858.

IP$_1$ Functional Assay and Schild Analysis. The activity of the TP receptor was measured by quantifying cellular levels of the IP3 metabolite, IP1, using a homogeneous time-resolved fluorescence (HTRF) assay kit (IP-One Tb, Cisbio, Bedford, MA). QBI-HEK 293A (MP Biomedicals, Solon, OH) cells were transfected with human or mouse TP receptor cDNA (α isoforms) that was cloned into the pcDNA5/TO vector (Invitrogen, Carlsbad, CA), and stable transformants were selected. Cells were plated at 10 000 cells/well into 384-well plates (Grenier Bio-One, Monroe, NC) in DMEM containing 4.5 g/L glucose (Invitrogen, Carlsbad, CA), 10% fetal bovine serum, L-glutamine, and penicillin/streptomycin, followed by incubation for 16 h at 37 °C with 5% CO$_2$. Culture media was removed and cells were then incubated for 15 min at 37 °C with 5% CO$_2$ in 10 mM Hepes, 1 mM CaCl$_2$, 0.4 mM MgCl$_2$, 4.2 mM KCl, 146 mM NaCl, 5.5 mM glucose, 50 mM LiCl, pH 7.4 (stimulation buffer) containing varying concentrations of test antagonist. I-BOP ([15-(1α,2β(5Z),3α-(1E,3S),4α)]-7-[3-hydroxy-4-(*p*-iodophenoxy)-1-butenyl-7-oxabicyclo-heptenoic acid) (Cayman Chemicals, Ann Arbor, MI) was added at concentrations indicated in the figure legends in stimulation buffer and incubated for 1 h at 37 °C with 5% CO$_2$. For Schild analyses, antagonist was added at fixed concentrations for 15 min in stimulation buffer, followed by a 1 h incubation with the varying concentrations of I-BOP. Following I-BOP incubation, D2-labeled IP$_1$ and Tb-labeled Anti-IP$_1$ cryptate were then added in lysis buffer per the manufacturer's instructions and incubated for 1 h at 25 °C. Plates were subsequently read on a Spectramax M5 microplate reader (Molecular Devices, Sunnyvale, CA). Data were expressed as the ratio of acceptor emission (665 nm) over donor emission (620 nm) following donor excitation (313 nm). For Schild analyses, the dose-ratio (DR) was defined as the ratio of the I-BOP EC$_{50}$ in the presence of a given concentration of antagonist to the I-BOP EC$_{50}$ in the absence of antagonist. If the antagonist competes with the agonist for receptor binding,

$$DR = 1 + [antagonist]/K_d$$

Thus, plotting the value of DR-1 vs the concentration of antagonist in a double log-plot generates a line with a slope of 1 where the *x*-intercept is equal to the K_d for the antagonist. Schild Analysis was performed in GraphPad Prism version 4 for Windows (GraphPad Software, San Diego, CA).

Aβ Secretion and APP Assays. QBI-HEK 293A cells stably expressing either mTP or hTP receptor were transfected with pcDNA3.1 (Invitrogen, Carlsbad, CA) containing a hygromycin selection cassette and the human APP695 cDNA, and stable transformants were selected (HEK293-TP/APP cells). Cells were plated into 96-well polystyrene plates at 20 000 cells/well in DMEM containing 4.5 g/L glucose (Invitrogen, Carlsbad, CA), 10% fetal bovine serum, L-glutamine, and penicillin/streptomycin, followed by incubation for 16 h at 37 °C with 5% CO$_2$. Media was aspirated and replaced with media containing 0.5% fetal bovine serum and test antagonist at varying concentrations. Cells were incubated with test antagonist for 1 h at 37 °C with 5% CO$_2$, followed by the addition of I-BOP at a final concentration as indicated in the figure legend, and the cells were incubated an additional 48 h at 37 °C with 5% CO$_2$. Aliquots of culture media were then removed for measurement of Aβ (1−40) and Aβ (1−42) levels by ELISA. Cell lysates were prepared by washing cells in PBS and then scraping cells into RIPA buffer (25 mM Tris, 150 mM NaCl, 1% NP-40, 1% sodium deoxycholate, 0.1% SDS, 0.1 mM PMSF, pH 7.6) containing protease inhibitor cocktail. Lysates were incubated on ice and vortexed every 10 min for 30 min, and then centrifuged at 13 000g for 30 min at 4 °C. The total protein concentration in the supernatant was detected by BCA assay (Thermo Scientific, IL), and 30 μg of total protein was separated by 10% SDS-PAGE and transferred to nitrocellulose membrane. Membranes were blocked in blocking buffer (LiCor Biosciences, Lincoln, NE), incubated overnight at 4 °C with primary antibody to detect the C-

937

dx.doi.org/10.1021/cn3000795 | *ACS Chem. Neurosci.* 2012, 3, 928−940

terminus of APP (5685) or tubulin (12G10), washed, incubated with IRDye 800CW or 680RD conjugated secondary antibodies, and imaged with the Odyssey imaging system (LI-COR Biosciences, Lincoln, NE). Blot quantification was performed using Image Studio (LI-COR Biosciences, Lincoln, NE).

Aβ ELISA. 384-well plates were coated with 10 μg/mL of Ban50 as a capture antibody and incubated overnight at 4 °C. Plates were blocked for a minimum of 3 days at 4 °C with Block-Ace (AbD Serotec, Raleigh, NC). Blocking solution was then removed, and media samples were diluted onto plates and incubated for 16 h at 4 °C. Plates were subsequently washed and incubated with the HRP-conjugated antibodies BA27 (Aβ(1−40)ELISA) or BC05 (Aβ(1−42)ELISA)[46] for 4 h at 25 °C and subsequently subjected to chemiluminescence detection.

APP Quantitative PCR. Cells were treated with I-BOP, or I-BOP and S18886, as described above, and mRNA was purified using a RNEasy kit (Qiagen, Venlo, Netherlands). The RNA was subjected to a single round of reverse transcription using the SuperScript III First-Strand Synthesis System (Invitrogen, Carlsbad, CA) to generate cDNA. For RT-PCR, 1 μL of cDNA was added to each well containing SYBR Green Master Mix (Invitrogen, Carlsbad, CA) and forward and reverse primers at a final concentration of 100 nM (APP) or 300 nM (GAPDH), which were the concentrations of primer sets determined to be 100% efficient. PCR was run on the Applied Biosystems 7500 Fast Real-time PCR system (Life Technologies, Foster City, CA) using the $\Delta\Delta C_t$ comparative method. Human APP cDNA was quantified and normalized to human GAPDH as an internal control. The primer sequences that were used are as follows:

hAPP forward: CCGCTCTGCAGGCTGTTC
hAPP reverse: GCGGACATACTTCTTTAGCATATTGA
hGAPDH forward: GAAGGTGAAGGTCGGAGTCAACG
hGAPDH reverse: CCAGAGTTAAAAGCAGCCCTGGTG

Radioligand Binding Assay. QBI-HEK 293A cells expressing hTP or mTP receptor were grown as described previously and harvested in phosphate-buffered saline with 1 mM EDTA. The cell pellet was homogenized in a glass homogenizer in 20 mM Hepes, 1 mM EGTA, and 0.5 mM DTT with protease inhibitor cocktail. The homogenate was initially centrifuged at 1000g for 10 min at 8 °C to remove cell debris. The resulting supernatant was then centrifuged in a Beckman L8−70 M ultracentrifuge (Beckman-Coulter, Brea, CA) at 21 000 rpm for 30 min at 4 °C, and the pellet was resuspended in 20 mM Hepes, 1 mM EGTA, and 100 mM NaCl. Protein level in the membrane preparation was determined with a BCA assay (Thermo-Fisher, Rockland, IL), and the samples were stored at −80 °C. Varying concentrations of ^{3}H-SQ29,548 (PerkinElmer, Waltham, MA) were incubated with 25 μg membrane in 50 mM Tris, 4 mM CaCl$_2$, 0.1% ascorbic acid, pH 7.5 for 2 h at 25 °C in 96-well polystyrene plates. Separation of bound from free radioligand was accomplished by rapid vacuum filtration onto 96-well GF/B filter plates (PerkinElmer, Waltham, MA). Filters were washed 8 times in 50 mM Tris, pH 6.9 and allowed to dry for 16 h. Plates were sealed and filters were dissolved in 50 mL of Betaplate Scintillation fluid (PerkinElmer, Waltham, MA), followed by analysis on a PerkinElmer 1450 LSC Microbeta Trilux scintillation counter (PerkinElmer, Waltham, MA). Nonspecific binding was determined by incubating ^{3}H-SQ29,548 at multiple concentrations in the presence of 100 μM cold SQ29,548.

Mouse Pharmacokinetics. One month old female B6C3F1 mice (Charles River Laboratories, Wilmington, MA) were administered 5 mg/kg compound in DMSO via an intraperitoneal (IP) injection (groups of 3 or more mice/tested compound). After 1 h, animals were anesthetized with ketamine/xylazine in accordance with protocols approved by the University of Pennsylvania and according to the NIH guide for the care and use of Laboratory Animals. Blood was collected via cardiac puncture, and animals were perfused with PBS. Plasma was separated from blood as described.[47] Brains were collected and prepared for compound quantification.

Compound Quantification in Tissues. Aliquots (50 μL) of mouse brain homogenate (1:2 w/v in 10 mM NH$_4$OAc, pH 5.7) or plasma were extracted with acetonitrile (1:5 v/v), centrifuged, and the supernatant removed for LC-MS/MS analysis (Waters Acquity UPLC-TQD, Milford, MA). Analytes were separated by reversed phase liquid chromatography using a water/acetonitrile/0.1% formic acid gradient and detected in the positive ion mode. Data were acquired using multiple reaction monitoring of compound specific collision-induced ion transitions. Standard curves were generated for each compound using spiked brain homogenate or plasma and extracted as above. Peak area was plotted against concentration and a linear regression curve was used to quantify the unknowns.

Determination of Compound Plasma and Brain Unbound Fraction. The unbound fractions of compound in mouse plasma and brain were determined using a rapid equilibrium dialysis as previously described.[47]

Data Analysis. Equilibrium dissociation constants (K_d), IC$_{50}$ values, and Schild intercepts were calculated with GraphPad Prism software (GraphPad Software Inc., La Jolla, CA).

■ AUTHOR INFORMATION

Corresponding Author
*Mailing address: Director of Drug Discovery, Center for Neurodegenerative Disease Research, Department of Pathology and Laboratory Medicine, University of Pennsylvania, 3600 Spruce St., Maloney 3rd Floor, Philadelphia, PA, 19104. Telephone: 01-215-615-5262. Fax: 01-215-349-5909. E-mail: kbrunden@upenn.edu.

Author Contributions
§These authors contributed equally to the manuscript.

Notes
The authors declare no competing financial interest.

■ ABBREVIATIONS

AD, Alzheimer's disease; APP, amyloid precursor protein; B/P, brain-to-plasma; HTRF, homogeneous time-resolved fluorescence; I-BOP, [1S-1α,2β(5Z),3α(1E,3R*),4α)]-7-[-3-(3-hydroxy-4-(4″-iodophenoxy)-1-butenyl)-7-oxabicyclo-[2.2.1]-heptan-2-yl]-5-heptenoic acid; IP, intraperitoneal; IP$_1$, inositol monophosphate; IP$_3$, inositol triphosphate; iPF2α, F2α-isoprostane; THN, tetrahydronaphthalene; TP, thromboxane A2-prostanoid

■ REFERENCES

(1) Mebane-Sims, I. (2009) 2009 Alzheimer's disease facts and figures. *Alzheimer's Dementia 5*, 234−270.
(2) Reitz, C., Brayne, C., and Mayeux, R. (2011) Epidemiology of Alzheimer disease. *Nat. Rev. Neurol. 7*, 137−152.
(3) Akiyama, H., Barger, S., Barnum, S., Bradt, B., Bauer, J., Cole, G. M., Cooper, N. R., Eikelenboom, P., Emmerling, M., Fiebich, B. L., Finch, C. E., Frautschy, S., Griffin, W. S. T., Hampel, H., Hull, M., Landreth, G., Lue, L. F., Mrak, R., Mackenzie, I. R., Mcgeer, P. L., O'Banion, M. K., Pachter, J., Pasinetti, G., Plata-Salaman, C., Rogers, J., Rydel, R., Shen, Y., Streit, W., Strohmeyer, R., Tooyoma, I, Van Muiswinkel, F. L., Veerhuis, R., Walker, D., Webster, S., Wegrzyniak, B., Wenk, G., and Wyss-Coray, T. (2000) Inflammation and Alzheimer's disease. *Neurobiol. Aging 21*, 383−421.
(4) De Strooper, B. (2010) Proteases and Proteolysis in Alzheimer Disease: A Multifactorial View on the Disease Process. *Physiol. Rev. 90*, 465−494.
(5) Kosik, K. S., Joachim, C. L., and Selkoe, D. J. (1986) Microtubule-Associated Protein Tau (Tau) Is A Major Antigenic Component of Paired Helical Filaments in Alzheimer-Disease. *Proc. Natl. Acad. Sci. U.S.A. 83*, 4044−4048.

(6) Lee, V. M. Y., Balin, B. J., Otvos, L., and Trojanowski, J. Q. (1991) A68 - A Major Subunit of Paired Helical Filaments and Derivatized Forms of Normal-Tau. *Science 251*, 675−678.

(7) Citron, M., Oltersdorf, T., Haass, C., Mcconlogue, L., Hung, A. Y., Seubert, P., Vigopelfrey, C., Lieberburg, I., and Selkoe, D. J. (1992) Mutation of the Beta-Amyloid Precursor Protein in Familial Alzheimers-Disease Increases Beta-Protein Production. *Nature 360*, 672−674.

(8) Haass, C., Lemere, C. A., Capell, A., Citron, M., Seubert, P., Schenk, D., Lannfelt, L., and Selkoe, D. J. (1995) The Swedish Mutation Causes Early-Onset Alzheimers-Disease by Beta-Secretase Cleavage Within the Secretory Pathway. *Nat. Med. 1*, 1291−1296.

(9) Mullan, M., Tsuji, S., Miki, T., Katsuya, T., Naruse, S., Kaneko, K., Shimizu, T., Kojima, T., Nakano, I., Ogihara, T., Miyatake, T., Ovenstone, I., Crawford, F., Goate, A., Hardy, J., Roques, P., Roberts, G., Luthert, P., Lantos, P., Clark, C., Gaskell, P., Crain, B., and Roses, A. (1993) Clinical Comparison of Alzheimers-Disease in Pedigrees with the Codon-717 Val-]Ile Mutation in the Amyloid Precursor Protein Gene. *Neurobiol. Aging 14*, 407−419.

(10) Tanzi, R. E., and Bertram, L. (2005) Twenty years of the Alzheimer's disease amyloid hypothesis: A genetic perspective. *Cell 120*, 545−555.

(11) Luo, Y., Bolon, B., Kahn, S., Bennett, B. D., Babu-Khan, S., Denis, P., Fan, W., Kha, H., Zhang, J. H., Gong, Y. H., Martin, L., Louis, J. C., Yan, Q., Richards, W. G., Citron, M., and Vassar, R. (2001) Mice deficient in BACE1, the Alzheimer's beta-secretase, have normal phenotype and abolished beta-amyloid generation. *Nat. Neurosci. 4*, 231−232.

(12) Lundkvist, J., and Naslund, J. (2007) gamma-Secretase: a complex target for Alzheimer's disease. *Curr. Opin. Pharmacol. 7*, 112−118.

(13) Sayre, L. M., Perry, G., and Smith, M. A. (2008) Oxidative stress and neurotoxicity. *Chem. Res. Toxicol. 21*, 172−188.

(14) Butterfield, D. A., Perluigi, M., and Sultana, R. (2006) Oxidative stress in Alzheimer's disease brain: New insights from redox proteomics. *Eur. J. Pharmacol. 545*, 39−50.

(15) Pratico, D., Clark, C. M., Lee, V. M. Y., Trojanowski, J. Q., Rokach, J., and FitzGerald, G. A. (2000) Increased 8,12-iso-iPF(2 alpha)-VI in Alzheimer's disease: Correlation of a noninvasive index of lipid peroxidation with disease severity. *Ann. Neurol. 48*, 809−812.

(16) Pratico, D., Lee, V. M. Y., Trojanowski, J. Q., Rokach, J., and FitzGerald, G. A. (1998) Increased F-2-isoprostanes in Alzheimer's disease: evidence for enhanced lipid peroxidation in vivo. *FASEB J. 12*, 1777−1783.

(17) Montine, T. J., Markesbery, W. R., Morrow, J. D., and Roberts, L. J. (1998) Cerebrospinal fluid F-2-isoprostane levels are increased in Alzheimer's disease. *Ann. Neurol. 44*, 410−413.

(18) Pratico, D., Uryu, K., Leight, S., Trojanowswki, J. Q., and Lee, V. M. Y. (2001) Increased lipid peroxidation precedes amyloid plaque formation in an animal model of Alzheimer amyloidosis. *J. Neurosci. 21*, 4183−4187.

(19) Breyer, R. M., Bagdassarian, C. K., Myers, S. A., and Breyer, M. D. (2001) Prostanoid receptors: Subtypes and signaling. *Annu. Rev. Pharmacol. Toxicol. 41*, 661−690.

(20) Huang, J. S., Ramamurthy, S. K., Lin, X., and Le Breton, G. C. (2004) Cell signalling through thromboxane A(2) receptors. *Cell. Signalling 16*, 521−533.

(21) Elmhurst, J. L., Betti, P. A., and Rangachari, P. K. (1997) Intestinal effects of isoprostanes: Evidence for the involvement of prostanoid EP and TP receptors. *J. Pharmacol. Exp. Ther. 282*, 1198−1205.

(22) Shineman, D., Zhang, B., Leight, S., Pratico, D., and Lee, V. (2008) Thromboxane receptor activation mediates isoprostane-induced increases in amyloid pathology in Tg2576 mice. *J. Neurosci. 28*, 4785−4794.

(23) Cimetière, B, Dubuffet, T, Muller, O, Descombes, J. J., Simonet, S, Laubie, M, Verbeuren, T. J., and Lavielle, G. (2008) Synthesis and biological evaluation of new tetrahydronaphthalene derivatives as thromboxane receptor antagonists. *Bioorg. Med. Chem. Lett. 8*, 1375−1380.

(24) Narumiya, S., and FitzGerald, G. A. (2001) Genetic and pharmacological analysis of prostanoid receptor function. *J. Clin. Invest. 108*, 25−30.

(25) Chaer, R. A., Graham, J. A., and Mureebe, L. (2006) Platelet function and pharmacologic inhibition. *Vasc. Endovasc. Surg. 40*, 261−267.

(26) Austin, R. P., Davis, A. M., and Manners, C. N. (1995) Partitioning of Ionizing Molecules Between Aqueous Buffers and Phospholipid-Vesicles. *J. Pharm. Sci. 84*, 1180−1183.

(27) Pajouhesh, H., and Lenz, G. R. (2008) Medicinal chemical properties of successful central nervous system drugs. *NeuroRx 2*, 541−553.

(28) Morinelli, T. A., Oatis, J. E., Okwu, A. K., Mais, D. E., Mayeux, P. R., Masuda, A., Knapp, D. R., and Halushka, P. V. (1989) Characterization of An I-125-Labeled Thromboxane-A2/Prostaglandin-H2 Receptor Agonist. *J. Pharmacol. Exp. Ther. 251*, 557−562.

(29) Lefer, D. J., Mentley, R. K., and Lefer, A. M. (1987) Protective Effects of A New Specific Thromboxane Antagonist in Arachidonate-Induced Sudden-Death. *Arch. Int. Pharmacodyn. Ther. 287*, 89−95.

(30) Knezevic, I., Borg, C., and Lebreton, G. C. (1993) Identification of Gq As One of the G-Proteins Which Copurify with Human Platelet Thromboxane-A2 Prostaglandin-H2 Receptors. *Blood 82*, A156.

(31) Dorn, G. W., Burch, R. M., Kochel, P. J., Mais, D. E., and Halushka, P. V. (1987) Decrease in Agonist Affinity for Human-Platelet Thromboxane-A2 Prostaglandin-H2 Receptors Induced by A Platelet-Derived Supernatant. *Biochem. Pharmacol. 36*, 1913−1917.

(32) Trachte, G. J. (1986) Thromboxane Agonist (U46619) Potentiates Norepinephrine Efflux from Adrenergic-Nerves. *J. Pharmacol. Exp. Ther. 237*, 473−477.

(33) Colquhoun, D. (2007) Why the Schild method is better than Schild realised. *Trends Pharmacol. Sci. 28*, 608−614.

(34) Giraldo, J., Serra, J., Roche, D., and Rovira, X. (2007) Assessing receptor affinity for inverse agonists: Schild and Cheng-Prusoff methods revisited. *Curr. Drug Targets 8*, 197−202.

(35) Funk, C. D., Furci, L., Moran, N., and FitzGerald, G. A. (1993) Point Mutation in the 7Th Hydrophobic Domain of the Human Thromboxane-A(2) Receptor Allows Discrimination Between Agonist and Antagonist Binding-Sites. *Mol. Pharmacol. 44*, 934−939.

(36) Barbu, E., Molnar, E., Tsibouklis, J., and Gorecki, D. C. (2009) The potential for nanoparticle-based drug delivery to the brain: overcoming the blood-brain barrier. *Expert. Opin. Drug Delivery 6*, 553−565.

(37) Chandra, A., Viswanathan, R., and Johnston, J. N. (2007) Synthesis of the ABC- and D-ring systems of the indole alkaloid ambiguine G. *Org. Lett. 9*, 5027−5029.

(38) Iida, S., and Togo, H. (2007) Direct oxidative conversion of alcohols and amines to nitriles with molecular iodine and DIH in aq NH3. *Tetrahedron 63*, 8274−8281.

(39) Demko, Z. P., and Sharpless, K. B. (2001) Preparation of 5-substituted 1H-tetrazoles from nitriles in water. *J. Org. Chem. 66*, 7945−7950.

(40) Dondoni, A., Fantin, G., Fogagnolo, M., Medici, A., and Pedrini, P. (1988) Thiazolylmethylenetriphenylphosporane and its benzo derivative: stable and practical wittig reagents for the synthesis of vinylthiazoles and vinylbenzo: two-carbon homologation of aldehydes. *Tetrahedron 44*, 2021−2031.

(41) Cimetière, B., Dubuffet, T, Muller, O, Descombes, J. J., Simonet, S, Laubie, M, Verbeuren, T. J., and Lavielle, G. (1998) Synthesis and biological evaluation of new tetrahydronaphthalene derivatives as thromboxane receptor antagonists. *Bioorg. Med. Chem. Lett. 8*, 1375−1380.

(42) Watts, I. S., Wharton, K. A., White, B. P., and Lumley, P. (1991) Thromboxane (Tx) A2 Receptor Blockade and Txa2 Synthase Inhibition Alone and in Combination - Comparison of Anti-Aggregatory Efficacy in Human Platelets. *Br. J. Pharmacol. 102*, 497−505.

(43) Thomas, D. W., Mannon, R. B., Mannon, P. J., Latour, A., Oliver, J. A., Hoffman, M., Smithies, O., Koller, B. H., and Coffman, T. M. (1998) Coagulation defects and altered hemodynamic responses in mice lacking receptors for thromboxane A(2). *J. Clin. Invest. 102*, 1994−2001.

(44) Hirata, T., Kakizuka, A., Ushikubi, F., Fuse, I., Okuma, M., and Narumiya, S. (1994) Arg(60) to Leu Mutation of the Human Thromboxane A(2) Receptor in A Dominantly Inherited Bleeding Disorder. *J. Clin. Invest. 94*, 1662−1667.

(45) Mumford, A. D., Dawood, B. B., Daly, M. E., Murden, S. L., Williams, M. D., Protty, M. B., Spalton, J. C., Wheatley, M., Mundell, S. J., and Watson, S. P. (2010) A novel thromboxane A(2) receptor D304N variant that abrogates ligand binding in a patient with a bleeding diathesis. *Blood 115*, 363−369.

(46) Gravina, S. A., Ho, L. B., Eckman, C. B., Long, K. E., Otvos, L., Younkin, L. H., Suzuki, N., and Younkin, S. G. (1995) Amyloid-Beta Protein (A-Beta) in Alzheimers-Disease Brain - Biochemical and Immunocytochemical Analysis with Antibodies Specific for Forms Ending at A-Beta-40 Or A-Beta-42(43). *J. Biol. Chem. 270*, 7013−7016.

(47) Brunden, K. R., Yao, Y., Potuzak, J. S., Ferrar, N. I., Ballatore, C., James, M. J., Hogan, A. L., Trojanowski, J. Q., Smith, A. B., 3, and Lee, V. M. Y. (2011) The characterization of microtubule-stabilizing drugs as possible therapeutic agents for Alzheimer's disease and related tauopathies. *Pharmacol. Res. 63*, 341−351.

■ NOTE ADDED AFTER ASAP PUBLICATION

After this paper was published on the Web July 27, 2012, a structure in Table 1 was corrected. The revised version was reposted August 28, 2012.